Phase imbalance impact on operating envelope for low-voltage distribution grid

Lionel Delchambre
ATM department & WET department
ULB & VITO
Brussels, Belgium
lionel.delchambre@ulb.be

Hamada Almasalma
WET department
VITO
Genk, Belgium
hamada.almasalma@vito.be

Patrick Hendrick
ATM department
ULB
Brussels, Belgium
patrick.hendrick@ulb.be

Pierre Henneaux
BEAMS department
ULB
Brussels, Belgium
pierre.henneaux@ulb.be

***Abstract*—Distribution System Operators must ensure safe operation of the Low Voltage distribution grid in the face of upcoming challenges posed by new assets (e.g. photovoltaic panels, electric vehicles) and new activities (e.g. energy sharing, frequency reserves). This task is further complicated by the fact that end-users may be unevenly connected to the phases without Distribution System Operators being aware of it. This can lead to unexpected voltage or current congestions. This paper presents an innovative method, a relaxed unbalanced three-phase optimal power flow, to compute the maximum day-ahead flexibility per end-user that can be unlocked while ensuring safe use of the low voltage grid, i.e. the operating envelope. Additionally, the paper shows results that controlling reactive power on the LV network could not increase flexibility potential and counteract imbalances caused by unevenly distributed phase connections.**

***Index Terms*—Operating Envelope, relaxed three-phases unbalanced optimal power flow, uneven distributed phase connections, low voltage flexibility**

I. Introduction

Distribution System Operators (DSOs) are facing upcoming challenges to ensure safe operation of the Low Voltage (LV) distribution grid. New assets such as photovoltaic panels (PV), heat pumps (HP) and electric vehicles (EV) are increasingly being installed, as well as new activities becoming available for LV assets, such as frequency reserves and energy sharing. Ensuring safe use of the grid is made more difficult by the fact that DSOs do not know which phase end-users are connected to, and phase connections can be highly unevenly distributed. This can lead to unexpected voltage or current congestions. When there is a congestion risk, DSOs need to define the maximum flexibility that can be unlocked by LV end-users while guaranteeing safe use of the grid by computing the day-ahead Operating Envelope (OE). In that context, the OE is defined as the maximum and minimum power available per end user while guaranteeing the absence of congestion (current and voltage) on the LV distribution grid.

To provide some background, OE principle is defined in 2009 in [1].The paper aimed to characterize the flexibility needed to include wind turbine generation in the California grid. Makarov's team publishes two years later a new paper considering load uncertainty in the model [2].

979-8-3503-9042-1/24/31.00©2024 IEEE

Later, [3] presented a method for assessing the *available* operational flexibility of a power system, compared to the previous concept of *needed* flexibility. This available flexibility is defined as the maximum technical capability of a single power system unit to modulate power and energy into the grid. The grid is considered as a copper plate and hence, internal constraints are not yet taken into account. For the LV loads and generators, five household appliances are considered and modeled in [4]: washing machines, tumble dryers, dishwashers, domestic boilers and EV.

The OE for power system is formally defined in [5]. The paper began with a state of the art on the principle of flexibility. It defined the flexibility at a certain time as the possible capacity of the system to provide flexible power for the next time steps. Flexibility is therefore represented in the form of a cone or an OE in a plan power versus time.

The OE concept is then used to ensure that load control does not exceed grid constraints. For example, [6] considered a building with PV, EV, thermal energy storage and HP and presents four strategies for controlling these LV loads and generators. An OE is then computed for each hourly electrical set point to assess the impact on the distribution grid constraints.

New methods are then used to compute the OE to reduce computation time, e.g. through probabilistic approach in [7] or through data-driven approach in [8]. The flexibility envelop concept is also applied on the distribution network in [9]. More recently, the OE is used to study the impacts of reconfiguration on the distribution network [10].

More recently, [11] performed a phase voltage sensitivity analysis of an unbalanced distribution network. The results concluded that congestion can occur even when all customers are within the limits of the single line OE and hence, imbalances cannot be neglected. In that context, [12] studied the calculation of OE for the integration of DER in unbalanced distribution networks. This is all the more relevant since today DSOs do not necessarily know to which phase end-users are connected and strong imbalances can be unexpectedly observed on the LV distribution network. Nevertheless, this paper considered only linearization to implement an unbalanced three-phases optimal power flow (UTOPF) for computing OE.

This paper complements the literature by presenting a

tractable and relaxed UTOPF with second-order conic relaxation. In addition, a case study with high imbalances highlights the impact of phase connection on the OE.

The remainder of the paper is organized as follows: Section II presents the relaxed and tractable UTOPF with SOCP relaxation, Section III presents the case study considering strong phase imbalances, Section IV presents the results and discussions and the last section ends with the conclusion.

II. Methodology to compute OE

A. Focus on relaxed UTOPF on BFM with SOCP relaxation

The methodology used to compute OE in this paper is an UTOPF. In general, the power flow equations used as constraints are quadratic non-convex. Therefore, tractability and time computation represent challenges. Several methods exist in the literature to convexify OPF equations [13]: approximation methods [14], machine learning methods, as presented in the introduction, but also relaxation methods [15].

Approximation and relaxation approaches are compared for multiphase distribution grid in [16]. The case studies presented in the paper prove that convex relaxation is numerically exact, while the linearized approximation using the Lindistflow model leads to low accuracy when imbalances are high. Because this paper aims to study a situation with strong imbalances, a relaxation method is preferred to a linearization method.

Regarding relaxation methods in general for OPF, paper [15] compares three convex relaxation methods: semi-definite (SDP), chordal (CP) and second-order cone (SOCP) relaxations. The exactness of these relaxations is discussed in [17] and more specifically for branching flow models in [18] and [19]. It is proven that for a radial network, SOCP relaxation should always be preferred because the solution is exact and it is the tightest and simplest relaxation of the three (SOCP, CP and SDP) [17].

Finally, PF equations can be modeled through Bus Injection Model (BIM) or Branch Flow Model (BFM). Branch Flow Model (BFM) is to be preferred to Bus Injection Model (BIM) because it is numerically more stable [15].

This paper therefore focuses on a relaxed UTOPF on BFM with SOCP relaxation.

B. Problem formulation

The real and imaginary parts must be considered separately for implementation purposes. The UTOPF equations with SOCP relaxations are inspired from paper [20] where shunt currents are neglected and the reduced serie impedance matrix presented in [21] is implemented. The notation considered is clarified in Table I.

Sets - Four sets are considered and represented in Table II). Note that for radial networks, $\{\mathcal{B}\} = \{\mathcal{N}\} + 1$.

Variables - Four lifted complex variables are defined for the problem and therefore eight variables in the real domain (see Table III).

TABLE I
Typography and mathematical notation

$\mathbb{R}^{n\times m}$	set of real $n \times m$ matrices
$\mathbb{C}^{n\times m}$	set of complex $n \times m$ matrices
$\mathbb{H}^n \in \mathbb{C}^{n\times n}$	set of Hermitian $n \times n$ matrices
X^*	Conjugate of X
$X^\intercal$	Transpose of X
$\circ$	Element-wise multiplication
diag(X)	Extract diagonal of X, diag: $\mathbb{C}^{n\times n} \rightarrow \mathbb{C}^{n\times 1}$
$\succeq$	Semi-definite positive operator

TABLE II
Sets and indices

Phases	$p, q \in \mathcal{P} = \{a, b, c\}$
Branches	$n \in \mathcal{N}$
Busses	$b \in \mathcal{B}$
End-users	$c \in \mathcal{C} \subset \mathcal{B}$

As an example, the lifted variable for the voltage satisfies the following equations. Lifted currents satisfy similar equations that are not described in this paper.

$$W_b = W_b^{re} + jW_b^{im} = U_b(U_b)^H, \tag{1}$$

$$W_b \succeq 0, rank(W_b) = 1. \tag{2}$$

The structure of W_b as a real-valued matrix in rectangular coordinates is expressed as Equation (3). Note that 9 unique scalar variables are required.

$$W_b = \begin{bmatrix} W_{b,aa}^{re} & W_{b,ab}^{re} & W_{b,ac}^{re} \\ W_{b,ab}^{re} & W_{b,bb}^{re} & W_{b,bc}^{re} \\ W_{b,ac}^{re} & W_{b,bc}^{re} & W_{b,cc}^{re} \end{bmatrix} + j \begin{bmatrix} 0 & W_{b,ab}^{im} & W_{b,ac}^{im} \\ -W_{b,ab}^{im} & 0 & W_{b,bc}^{im} \\ -W_{b,ac}^{im} & -W_{b,bc}^{im} & 0 \end{bmatrix} \tag{3}$$

It is important to note that the variables are not the voltage, current and power phasors, but the outer product of voltage phasors $W_b = v_b * v_b^H$, current phasors $L_n = i_n * i_n^H$ and then $S_n = v_n * i_n^H$, where H denotes the Hermitian matrix. Indeed, this paper considers lifted variables with higher dimension to linearize some of the constraints. Nevertheless, to guarantee that a solution to the original problem can be recovered, two types of constraints need to be added: the positive semidefinite constraint and the rank-1 constraint.

Parameters - Parameters are listed in table IV. One important parameter is the series impedance matrix z_n which characterizes the self and mutual impedance between the

TABLE III
Lifted optimization variables

	Complex domain	Real domain
Power branch (W)	$S_n \in \mathbb{C}^{\lvert\mathcal{P}\rvert\times\lvert\mathcal{P}\rvert}$	$P_n, Q_n \in \mathbb{R}^{\lvert\mathcal{P}\rvert\times\lvert\mathcal{P}\rvert}$
Power busses (W)	$s_b \in \mathbb{C}^{\lvert\mathcal{P}\rvert\times 1}$	$p_b, q_b \in \mathbb{R}^{\lvert\mathcal{P}\rvert\times 1}$
Branch current product (A^2)	$L_n \in \mathbb{C}^{\lvert\mathcal{P}\rvert\times\lvert\mathcal{P}\rvert}$	$L_n^{Re}, L_n^{Im} \in \mathbb{H}^{\lvert\mathcal{P}\rvert\times\lvert\mathcal{P}\rvert}$
Bus voltage product (V^2)	$W_b \in \mathbb{C}^{\lvert\mathcal{P}\rvert\times\lvert\mathcal{P}\rvert}$	$W_b^{Re}, W_b^{Im} \in \mathbb{H}^{\lvert\mathcal{P}\rvert\times\lvert\mathcal{P}\rvert}$

TABLE IV
PARAMETERS

Bus voltage magnitude min./max. (V)	$U_b^{min}, U_b^{max} \in \mathbb{R}^{\lvert\mathcal{P}\rvert\times 1}$
Branch current rating (A)	$I_n^{ampacity} \in \mathbb{R}^{\lvert\mathcal{P}\rvert\times 1}$
Branch apparent power rating (VA)	$S_n^{rate} \in \mathbb{R}^{\lvert\mathcal{P}\rvert\times 1}$
Branch series impedance (Ω)	$z_n \in \mathbb{R}^{\lvert\mathcal{P}\rvert\times\lvert\mathcal{P}\rvert}$
End-user active power bound (W)	$P_c^{min}, P_c^{max} \in \mathbb{R}^{\lvert\mathcal{P}\rvert\times 1}$
End-user reactive power bound (var)	$Q_c^{min}, Q_c^{max} \in \mathbb{R}^{\lvert\mathcal{P}\rvert\times 1}$

cables within the feeder. The reduced model presented in [21] is considered for this paper.

Constraints - Constraints are expressed hereafter:

$$W_n = W_{\pi_n} + Z_n L_n Z_n^H - S_n Z_n^H - Z_n S_n^H \tag{4}$$

$$dg(S_n - Z_n L_n) + s_n = \sum_{k:n\to k} dg(S_k) \tag{5}$$

$$M = \begin{bmatrix} W_{\pi_n} & S_n \\ S_n^* & L_n \end{bmatrix} \succeq 0 \tag{6}$$

$$0 \leq diag(S_n) \circ diag(S_n)^* \leq S_n^{rate} \circ S_n^{rate} \tag{7}$$

$$P_c^{min} \leq p_c - p_{c,conso} \leq P_c^{max} \tag{8}$$

$$Q_c^{min} \leq q_c - q_{c,conso} \leq Q_c^{max} \tag{9}$$

$$U_b^{min} \circ U_b^{min} \leq diag(W_b^{re}) \leq U_b^{max} \circ U_b^{max} \tag{10}$$

$$-U_b^{max}(U_b^{max})^\intercal \leq W_b^{re}, W_b^{im} \leq U_b^{max}(U_b^{max})^\intercal \tag{11}$$

$$I_n^{min} \circ I_n^{min} \leq diag(L_n^{re}) \leq I_n^{max} \circ I_n^{max} \tag{12}$$

$$-I_n^{max}(I_n^{max})^\intercal \leq L_n^{re}, L_n^{im} \leq I_n^{max}(I_n^{max})^\intercal \tag{13}$$

Ohm's law and power balance equations are defined respectively in Equation (4) and Equation (5), expressed in the complex domain. Note that these constraints only apply on the diagonal elements.

An additional auxiliary constraint is considered to constrain lifted voltages, lifted currents and power branches in Equation (6). This additional constraint comes from lifting the variables to guarantee to recover a solution to the original problem. Note that only the PSD constraint is considered, because the rank-1 constraint, that is non-convex, is removed due to the SOCP relaxation.

Finally, injection constraints are added to the problem with Equations (7), (8) and (9) and network constraints respectively for voltage limits, with Equations (10) and (11), and current limits, with Equations (12) and (13).

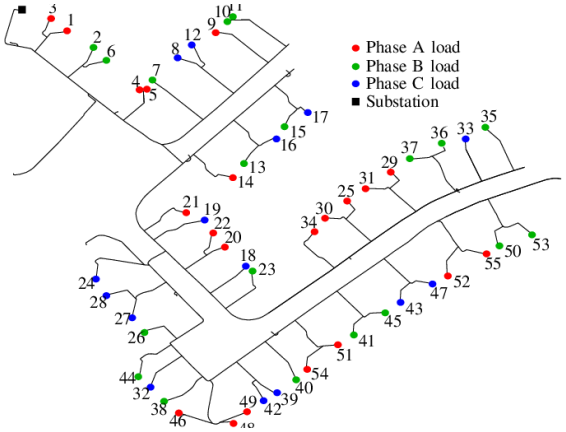

Fig. 1. Reduced IEEE European LV Testfeeder with phase connection

III. Case Study

This section first presents the benchmark grid studied, then the objective function implemented and finally presents the end-users load profiles.

A. Grid and phase connection

The reduced IEEE European LV Testfeeder is selected for the case study [22]. This grid is represented in Fig. 1 with 55 end-users and their initial phase connections. Each end-user is connected to the grid with a maximum power capacity (in this case: $\pm 9.2kVA$ for a monophase 40A). In the results, a worst-case is considered with all end-users connected to the same phase, in order to highlight the worst and unrealistic unbalance case. Although it is unlikely that all end-users will be connected to the same feeder, DSOs currently do not necessarily know which phase the end user is connected to and unexpected imbalances can arise.

B. Objective function

A single objective function is implemented to focus on this paper objectives. The objective function optimizes the sum of active powers per household, minus losses to ensure the existence of an exact solution. This objective function should maximize the available flexibility, but it will be heterogeneously distributed among end-users. To compute the upper and lower flexibility envelopes, the objective function switches from maximization to minimization.

$$max \sum_{i\in\mathcal{C}} p_{i,\phi} - \lambda \sum_{n\in\mathcal{N}} diag(r_n L_n^{Re}) \tag{14}$$

C. End-users load profile

The load profiles, active and reactive power, considered in this paper are deterministic and come from the benchmark grid for a specific moment in the time series (12:00). This paper does not aim to further refine the calculation of load profiles. However, two assumptions are considered for the reactive power of the OE: the reactive power per end user can either remain variable or be constrained to a fixed power factor (here, PF = 1, as analyzed from real grid data in [23]).

D. Implementation

The problem is implemented in python, using the cvxpy software-based optimization language and the MOSEK solver. This choice is mainly motivated by the need for the software and the solver to support the SDP constraint.

IV. Results and discussion

In this paper, the maximum (minimum) power available on the feeder is calculated by summing the maximum (minimum) power of each end user. Active power set points constitute the OE and are computed for each end-user for the four case studies. Fig. 3 shows the upper and lower OE for each end-user when the PF can vary. In this situation, the reactive power is considered a variable and is only limited by the maximum current that can be yield through the injection connection. The blue curve (OE1) represents the initial scenario in which end-users are located on different phases, and the green curve (OE2) represents the scenario in which all end-users are located on the same phase. The comparison between OE1 and OE2 shows that connecting all end users to the same phase results in a reduction of the OE. Fig. 4 similarly shows two upper and lower OE (OE3 and OE4) and shows that connecting all end users to the same feeder reduces the available flexibility. The difference between the two figures is that in the second figure the PF is fixed. By summing the maximum (minimum) power value for all end-users connected to the feeder, these figures show that for OE1, the maximum active power available on the LV feeder is 446 kW and the minimum power is -384.2 kW, for OE2, 159.06 kW and -151.18 kW, for OE3 445.98 kW and -384.11 kW, and for OE4 159.06 kW and -151.18 kW.

The statistical data for each OE are summarized in Fig. 2 where OE1 represents the initial case study with variable PF, OE2 where all end-users are on the same phase with variable PF. OE3 and OE4 are both for fixed PF and represent respectively the initial situation and the situation where all end-users are on the same feeder.

The typology of the grid as well as phase connections influence the results. Indeed, when looking at the end of the feeder for the longest branch (on the left right of the Fig. 1), end-users 52 and 55 on phase A and 50 and 53 on phase B corresponds to the most constrained end-users in OE1 and OE3. End-user 51 seems to be an exception, which is related to the length of the cable connecting the end-user to the grid. Indeed, end-user 51 is connected with a 3.2 m cable to the grid, whereas end-user 54 is connected with an 8 m cable. When considering strong imbalances, end-users closer to the substation also access more flexibility than end-users located to the end of the feeder. Hence, the further end-users are located from the substation and the more loaded the phase, the more constrained the end-users are.

This paper also presents the influence of controlling reactive power on the OE. Indeed, today, if an end-user injects or consumes, it is likely that it will involve electronic equipment (e.g. inverters for PV, EV, domestic batteries) that has the possibility of modifying the reactive power command. The results show that if the PF is set to a fixed value and end-users are connected evenly among phases, when comparing OE1 and OE3, the magnitude of available flexibility is similar than when PF can vary. Similarly, when comparing OE2 and OE4, available flexibility is not influenced by reactive power control. Therefore, reactive power control cannot increase flexibility envelope or compensating for strong imbalances.

A final result to be discussed is the computation time to obtain the result for a single upper or lower OE. The relaxed UTOPF with SOCP relaxation implemented on python runs between 31 and 36 seconds, for this grid with 55 end-users. If the tool is to be applied for a full distribution network, with millions of end-users, and the computation time scales proportionally to the number of end-users, this tool is not relevant to be used for intra-day operations. Indeed, for these applications, results must be obtained within 15 or 30 minutes. However, the relaxed UTOPF with SOCP relaxation could be used for static or day-ahead applications where several hours is an acceptable time frame to obtain results.

V. Conclusion

In conclusion, this paper first presents a relaxed UTOPF with SOCP relaxation on a LV distribution network for day-ahead applications. Furthermore, this paper presents the effect of strong imbalances and of controlling reactive power on OEs. This shows that strong imbalances reduce the OE and that controlling reactive power on the LV network could not increase flexibility potential and counteract imbalances.

Further work could consider the stochasticity of end-user load profiles to obtain a more realistic OE, as well as the probability that an end-user is connected to a specific phase, as DSOs do not necessarily have this information. Other objective functions could also be considered, to better understand the principle of fairness for example (such as ensuring that all end-users have access to the same power).

Acknowledgment

This study is conducted under the framework of the federal Belgian project named ALEXANDER, funded by the Transition Energy Fund.

References

[1] Y.V. Makarov, C. Loutan, J. Ma, P. de Mello, "Operational Impacts of Wind Generation on California Power Systems", IEEE Transactions on Power Systems, Vol. 24, pp. 1039-1050, 2009.

[2] Y.V. Makarov, P.V. Etingov, J. Ma, Z. Huang, K. Subbarao, "Incorporating Uncertainty of Wind Power Generation Forecast Into Power System Operation, Dispatch, and Unit Commitment Procedures", IEEE Transactions on Sustainable Energy, Vol. 2, pp. 433-443, 2011.

[3] A. Ulbig, G. Andersson, "On operational flexibility in power systems", 2012 IEEE Power and Energy Society General Meeting, 2012.

[4] R. D'hulst, W. Labeeuw, B. Beusen, S. Claessens, G. Deconinck, K. Vanthournout, "Demand response flexibility and flexibility potential of residential smart appliances: Experiences from large pilot test in Belgium", Applied Energy, Vol. 155, pp. 79-90, 2015.

[5] H. Nosair, F. Bouffard, "Flexibility Envelopes for Power System Operational Planning", IEEE Transactions on Sustainable Energy, vol. 6, pp. 800-809, 2015.

[6] J. Gasser, H. Cai, S. Karagiannopoulos, P. Heer, G. Hug, "Predictive energy management of residential buildings while self-reporting flexibility envelope", Applied Energy, Vol. 288, 2021.

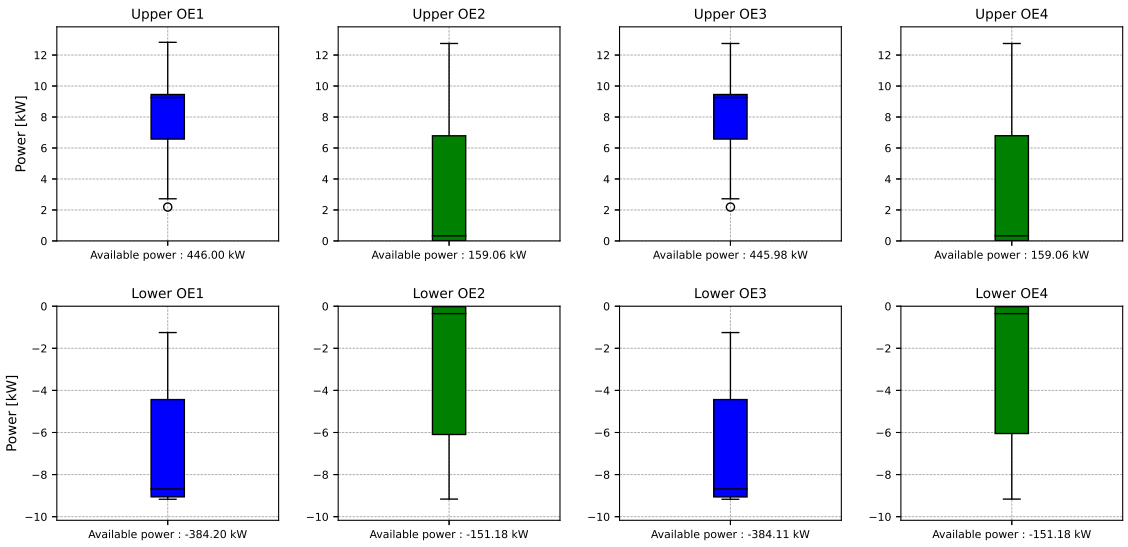

Fig. 2. Summary of the four upper and lower OE

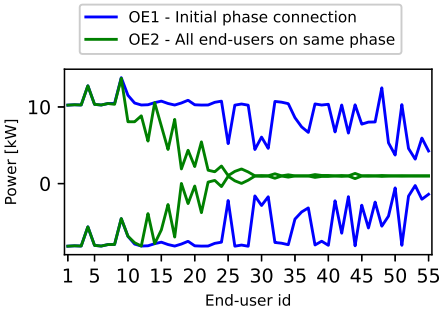

Fig. 3. Two inferior and superiors OE with variable PF where end-users are connected on different phases (blue) and to the same phase (green)

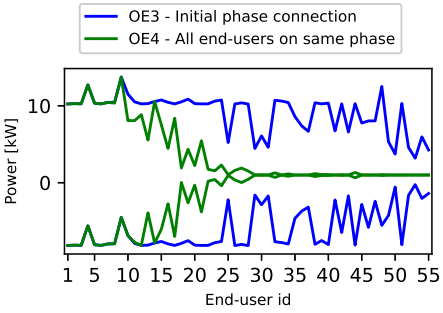

Fig. 4. Two inferior and superiors OE with fixed PF (PF=1) where end-users are connected on different phases (blue) and to the same phase (green)

[7] H. Nosair, F. Bouffard, "Economic Dispatch Under Uncertainty: The Probabilistic Envelopes Approach", IEEE Transactions on Power Systems, vol. 32, pp. 1701-1710, 2017.

[8] N. Hekmat, H. Cai, T. Zufferey, G. Hug, P. Heer, "Data Driven Demand-Side Flexibility Quantification: Prediction and Approximation of Flexibility Envelopes", arxiv, 2022.

[9] Y. Huo, Yuchong, F. Bouffard, G. Joós, "Flexibility Envelopes for Distribution Networks", 2018 IEEE Power & Energy Society General Meeting (PESGM), 2018.

[10] A. Churkin, M. Sanchez-Lopez, M.I. Alizadeh, F. Capitanescu, E.A.M. Ceseña, P. Mancarella, "Impacts of Distribution Network Reconfiguration on Aggregated DER Flexibility", arxiv, 2023.

[11] B. Liu, J. H. Braslavsky, "Sensitivity and Robustness Issues of Operating Envelopes in Unbalanced Distribution Networks," IEEE Access, vol. 10, pp. 92789-92798, 2022.

[12] B. Liu, J.H. Braslavsky, "Robust Operating Envelopes for DER Integration in Unbalanced Distribution Networks", arxiv, 2022.

[13] Daniel K. Molzahn; Ian A. Hiskens, A Survey of Relaxations and Approximations of the Power Flow Equations, now, 2019.

[14] J. Huang, B. Cui, X. Zhou and A. Bernstein, "A Generalized LinDist-Flow Model for Power Flow Analysis," 2021 60th IEEE Conference on Decision and Control (CDC), Austin, TX, USA, 2021, pp. 3493-3500.

[15] S. H. Low, "Convex Relaxation of Optimal Power Flow—Part I: Formulations and Equivalence," in IEEE Transactions on Control of Network Systems, vol. 1, no. 1, pp. 15-27, March 2014.

[16] L. Gan and S. H. Low, "Convex relaxations and linear approximation for optimal power flow in multiphase radial networks," 2014 Power Systems Computation Conference, Wroclaw, Poland, 2014, pp. 1-9.

[17] S. H. Low, "Convex Relaxation of Optimal Power Flow—Part II: Exactness," in IEEE Transactions on Control of Network Systems, vol. 1, no. 2, pp. 177-189, June 2014.

[18] M. Farivar and S. H. Low, "Branch Flow Model: Relaxations and Convexification—Part I," in IEEE Transactions on Power Systems, vol. 28, no. 3, pp. 2554-2564, Aug. 2013.

[19] N. Li, L. Chen and S. H. Low, "Exact convex relaxation of OPF for radial networks using branch flow model," 2012 IEEE Third International Conference on Smart Grid Communications (SmartGridComm), Tainan,Taiwan, 2012, pp. 7-12

[20] F. Geth and H. Ergun, Real-Value Power-Voltage Formulations of, and Bounds for, Three-Wire Unbalanced Optimal Power Flow, arxiv, August 2023

[21] A. Koirala, R. D'hulst, D. Van Hertem, Impedance modelling for European style Distribution Feeder, 2019 International Conference on Smart Energy Systems and Technology (SEST), September 2019.

[22] M.A. Khan, B. Hayes, A Reduced Electrically-Equivalent Model of the IEEE European Low Voltage Test Feeder, TechRxi, Preprint, 2021

[23] M. Vanin, H. Ergun, R. D'Hulst, K. Vanthournout, D. Van Hertem, Analysis and insights from reactive power measurements of low voltage users, 27th International Conference on Electricity Distribution (CIRED 2023),2023